Theories of the Nuclear Surface

LAWRENCE WILETS*

The Institute for Advanced Study, Princeton, New Jersey

I. EXPERIMENTAL REVIEW

QUANTITIES which theories of the nuclear surface seek to describe include the following: (1) surface thickness, (2) surface energy, (3) relative extent of neutrons and protons, and (4) extent of nuclear forces compared with matter. There now exists experimental information bearing on all of these, although some of it is still preliminary. All lengths are quoted in units of 10^{-13} cm$=1$ fermi (f).

(1) On the basis of the Stanford electron scattering experiments,[1,2] the nuclear charge distribution may be described as possessing a central region of rather uniform density (although a few percent central depression or rise is not ruled out) and a surface region in which the density falls from 90 to 10% of the central value in a distance $D=2.4$ f (accuracy about 10%) independent of nuclear mass number A. The density distribution is usually described by the function

$$\rho=\rho_0[1+e^{(r-R)/a}]^{-1}, \tag{1}$$

where $D=4.39a$. The precise functional form is not significant, but rather just two parameters, taken to be the half-density radius R and the falloff distance a or D. To a first approximation this is also the distribution of neutrons (the two together forming the matter distribution) but differences between the two distributions are of considerable interest.

The Stanford scattering experiments also show that the proton has a structure.[1,3] The charge distribution has been described by the form factor $\exp(-r/b)$, $b=0.23$ f. Various workers[4] have pointed out that the charge distribution should be a convolution of the distribution of the proton mass centers and the charge distribution of the proton. For a large nucleus the radius associated with the nuclear charge distribution is nearly equal to the radius of the mass-center distribution, but the surface thickness of the mass-center distribution, D_0, is less than that of the charge distribution,

$$D_0\approx D-4b^2/a\approx 2.0 \text{ f}. \tag{2}$$

Nuclear distortions or surface vibrations lead to an effective surface diffuseness greater by the order of βR than what we may call the intrinsic thickness. (β is a measure of nuclear deformation, roughly the difference between the semimajor and semiminor axes divided by the mean radius.) The results quoted in the foregoing are obtained from nuclei near closed shells and therefore have no static deformations. Even near closed shells, however, some surface thickening may result from surface vibrations. We give no estimate of the effect here, since near closed shells the nature of the collective motion has not been clearly established.

(2) The usual Weizsäcker semiempirical mass formula contains a term which varies as $A^{\frac{2}{3}}$ that is identified with the nuclear surface energy. Surface energy is also a function of the neutron excess, however, and more recent mass formulas have included a surface symmetry term which gives some small improvement in fits to mass data. Quantities in the mass formula needed later are defined by

$$\text{binding energy}=\left[E_v+E_{v,\,sy}\frac{(N-Z)^2}{A^2}\right]A+\left[E_s+E_{s,\,sy}\frac{(N-Z)^2}{A^2}\right]A^{\frac{2}{3}}+\text{Coulomb energy}+\mathcal{O}(A^{\frac{1}{3}}). \tag{3}$$

Values which Green[5] and Cameron[6] give for these quantities are listed in Table I. The variation in the

TABLE I.[a]

	Green[b]	Cameron-Green[c]	Cameron[d]
E_v	−15.83	−16.34	−17.04
$E_{v,\,sy}$	23.52	30.34	31.45
E_s	17.97	20.96	25.84
$E_{s,\,sy}$	0	−36.35	−44.24
n	1.28	1.16	1.01
ζ	0.38	0.49	0.72
K	175	218	302

[a] Values above the line are from semiempirical mass formulas, as defined in Eq. (3). The parameters below the line are derived from Eqs. (28), (31), and (32) using the added values $r_0=1.07$ f and $D=2.4$ f. All energies are in Mev; n and ζ are dimensionless.
There is a progressive error in the last column ($n=1$) of Table I, reference 17, which results in an understimate of nuclear compressibility. The derived falloff distance should be $D=2.0$ f; the subsequent interpolation to the observed falloff distance then leads to higher compressibility, compatible with the table given here.
[b] See reference 5.
[c] This column represents a regrouping by Green[5] of terms in Cameron's formula[6] such that terms of order $A^{\frac{1}{3}}$ do not appear explicitly. The coefficients were fixed by a least squares analysis.
[d] See reference 6.

* On leave from the University of California's Los Alamos Scientific Laboratory, Los Alamos, New Mexico.

[1] R. Hofstader, Revs. Modern Phys. **28**, 214 (1956).
[2] D. L. Hill and K. W. Ford, Ann. Revs. Nuclear Sci. **5**, 25 (1956).
[3] Yennie, Lévy, and Ravenhall, Revs. Modern Phys. **29**, 144 (1957).
[4] D. G. Ravenhall, Stanford Conference on Nuclear Sizes and Density Distributions (1957).
[5] A. E. S. Green, Revs. Modern Phys. **30**, 569 (1958); Phys. Rev. **95**, 1006 (1954); also private communication.
[6] A. G. W. Cameron, Can. J. Phys. **35**, 1021 (1951).

parameters among the various formulas indicates that a fair margin of choice is possible. Although all three of the formulas give good fits to empirical masses, differences in the parameters are of significance in the theoretical interpretation of surface effects. The surface energy may be expressed in terms of the surface tension parameter S, which has dimensions energy÷area,

$$E_s=4\pi r_0^2 S, \tag{4}$$

where the nuclear radius is given by $R=r_0A^{\frac{1}{3}}$.

(3) Direct measurements of the neutron density distribution remain very difficult, although there is some hope of distinguishing a difference between neutron and proton distributions. The best determination of a neutron-proton radius difference has been made by Abashian, Cool, and Cronin[7] utilizing the asymmetry between neutrons and protons in scattering by π^- and π^+ mesons. These experiments indicate only a small difference in the radii of the distributions with the protons slightly more extended. The numbers given are

$$R_p-R_n=(0.3\pm0.3)\text{ f}. \tag{5}$$

(4) Analyses of neutron and proton nuclear scattering experiments in terms of the optical model yield parameters characterizing the nuclear potential. While both neutron and proton scattering experiments give similar parameters, the proton experiments are generally more precise. Because a large number of parameters (from four on up) are available, there is about 4% margin of choice in the radial parameter. There is also some arbitrariness in the representation of the radius as a function of A. The point of view taken in this paper is that the difference between the potential radius and the matter radius is independent of A and will be evaluated for heavy nuclei.[8–10] This gives

$$R_v-R_m=(1.0\pm0.3)\text{ f}. \tag{6}$$

The potential surface thickness is given by $D=2.85$ f, or $a=(0.65\pm0.05)$ f.

II. THEORETICAL CONSIDERATIONS

A complete theory of the nuclear surface must deal with all of the complications of the finite nuclear many-body problem. Such a theory is not available in calculable form, but there remain nevertheless semi-empirical models which give insight into the physical problem and correlate quantitatively the above surface quantities with other observable nuclear properties. We return to the basic question of a theory from first principles in Sec. VII.

In order to isolate surface effects, it is frequently useful to consider a semi-infinite nuclear medium bounded by a plane surface. This permits investigation of the four quantities listed above, but neglects specific shell effects which may be important in the real nuclei. The inclusion of Coulomb energy also requires special consideration.

It is useful to have available a definition of the surface energy in the semi-infinite model to identify with S of Eq. (4). This quantity is given by the difference per unit area between the energy of the medium and the energy the same number of particles would have if all were located in the asymptotic (normal density) region of the nucleus,

$$\begin{aligned} S&=\int_{-\infty}^{\infty}\left\{\mathcal{E}(x)-\frac{\mathcal{E}_0}{\rho_0}\rho(x)\right\}dx \\ &=\mathcal{E}_0\int_{-\infty}^{\infty}\left\{\frac{\mathcal{E}(x)}{\mathcal{E}_0}-\frac{\rho(x)}{\rho_0}\right\}dx, \end{aligned} \tag{7}$$

where $\mathcal{E}_0=\mathcal{E}(-\infty)$ and $\rho_0=\rho(-\infty)$. The x direction is taken normal to the nuclear surface with the nuclear density falling off toward positive x values. The integrals are convergent for properly saturating nuclear forces. The quantity $\mathcal{E}(x)$ is the energy density (dimensions: energy÷volume) of the nuclear medium. $\mathcal{E}_0/\rho_0$ is the average binding energy per particle for an infinite nucleus, and is to be identified with the coefficient E_v of the term linear in A in the mass formulas (3). $\rho_0=(4\pi r_0^3/3)^{-1}$ can be obtained from the Stanford scattering experiments. Thus only the functional dependence of $\mathcal{E}(x)$ and $\rho(x)$ and not their absolute magnitudes are required to determine S. Such considerations make a semiempirical model of the nuclear surface feasible.

III. INDEPENDENT PARTICLE MODEL

That the nucleus should have finite surface thickness and surface energy follows from simple wave mechanical considerations, as pointed out by Bethe and Bacher,[11] Feenberg,[12] and others. Swiatecki's[13] development, which is the most complete, is followed closely in this section. In analogy with the nuclear shell model, it is assumed that in the first approximation the nucleons can be treated as moving in a given external potential. The external potential which Swiatecki considers contains a constant region plus a linearly increasing region. The slope is a parameter which can, for self-consistency, be adjusted to yield minimum surface energy.

Deviations of the wave function from that of in-

[7] Abashian, Cool, and Cronin, Phys. Rev. **104**, 855 (1956). See also W. N. Hess and B. J. Moyer, Phys. Rev. **101**, 337 (1956); R. W. Williams, Phys. Rev. **98**, 1387 (1955).

[8] Melkanoff, Moszkowski, Nodvik, and Saxon, Phys. Rev. **101**, 507 (1956).

[9] S. Fernbach, Revs. Modern Phys. **30**, 414 (1958).

[10] A. E. Glassgold, Revs. Modern Phys. **30**, 419 (1958).

[11] H. A. Bethe and R. F. Bacher, Revs. Modern Phys. **8**, 83 (1956), especially p. 164.

[12] E. Feenberg, Phys. Rev. **60**, 204 (1941).

[13] W. J. Swiatecki, Proc. Phys. Soc. (London) **A64**, 226 (1951); Phys. Rev. **98**, 203 (1955); Proc. Phys. Soc. (London) **A68**, 285 (1955); unpublished formulas and graphs in connection with lectures held during 1956–1957 at The Institute of Physics, University of Aarhus, Denmark.

dependent particles could, in principle, be treated by perturbation theory, but in the case of strong or singular potentials the expansion may be either slowly convergent or nonconvergent. Nevertheless, insight into the problem may be gained by using well-behaved potentials which reproduce low-energy nucleon-nucleon properties and yield the proper nuclear binding energy $E_v=\mathcal{E}_0/\rho_0$. The discussion here does not go beyond first order.

Consider first a potential well bounded by an infinitely high plane wall:

$$V(x)=\begin{cases}0, & x\leq 0,\\ \infty, & x>0.\end{cases} \tag{8}$$

The independent particle wave functions are

$$\psi_{k_1k_2k_3}=2^{\frac{1}{2}}\sin k_1x\,\exp i(k_2y+k_3z). \tag{9}$$

If the states are filled four each up to the Fermi momentum $\hbar K$, the density will be given by

$$\rho(x,y,z)=\rho(x)=\frac{4}{(2\pi)^3}\int\int\int|\psi_{k_1k_2k_3}|^2dk_1dk_2dk_3 \tag{10}$$
$$=\rho_0\{1+\tfrac{3}{4}X^{-2}\cos 2X-\tfrac{3}{8}X^{-3}\sin 2X\},$$

where $X=Kx$ and $\rho_0=\rho(-\infty)=2K^3/3\pi^2$. The function $\rho(x)$ is given in Fig. 1 ($x_0=0$). The mean position of the surface is given by $-b$, where

$$b=\int_{-\infty}^{0}\{1-\rho(x)/\rho_0 dx\}=3\pi/(8K). \tag{11}$$

The surface thickness is characterized by the wavelength of the most energetic particle, $\lambda\!\!\!^{-}=K^{-1}$, which for a Fermi energy of 32.5 Mev is 0.8 f. Because the density oscillates, the 90–10% falloff distance is not appropriate.

The kinetic energy density is given by

$$t(x,y,z)=t(x)=\frac{4}{(2\pi)^3}\int\int\int\psi^*\left(\frac{-\hbar^2}{2M}\nabla^2\right)\psi dk_1dk_2dk_3$$
$$=t_0\left\{1+\frac{5}{4}X^{-2}\cos 2X-\frac{15}{8}X^{-3}\sin 2X\right.$$
$$\left.-\frac{15}{8}X^{-4}\cos 2X+\frac{15}{16}X^{-5}\sin 2X\right\}, \tag{12}$$

while the surface kinetic energy, according to Eq. (7), is given by

$$T_s=t_0\int_{-\infty}^{0}\left\{\frac{t(x)}{t_0}-\frac{\rho(x)}{\rho_0}\right\}dx=t_0 2\pi/(32K), \tag{13}$$

where $t_0=t(-\infty)=0.6T_F\rho_0$ and

$$T_F=\hbar^2K^2/2M. \tag{14}$$

The surface kinetic energy for the infinite well is positive. Swiatecki ascribes this to the more effective penetration of the surface region by faster particles.

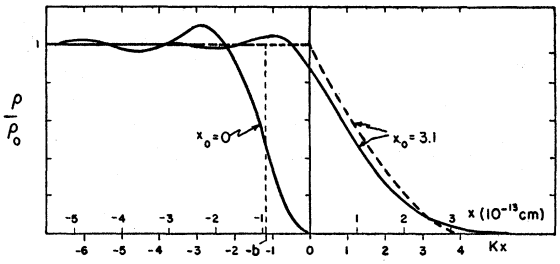

FIG. 1. Independent particle model: nuclear densities in a semi-infinite well with sloping wall (after Swiatecki[13]). The Fermi energy is 32.5 Mev ($K=1.25$ f^{-1}). The curve marked $x_0=0$ is for a vertical wall; the position of the mean density radius is marked by $-b$. The broken curve labeled $x_0=3.1$ is the Thomas-Fermi distribution.

Now consider the more general potential,

$$V(x)=\begin{cases}0, & x\leq 0,\\ T_F\dfrac{x}{x_0}, & x>0.\end{cases} \tag{15}$$

The independent particle wave functions for this potential can be written down as trigonometric functions in the constant potential region and Bessel functions of order $\frac{1}{3}$ in the linear region. Swiatecki[13] has obtained the density and surface kinetic energy for this problem exactly; we refer only to his results here. However, in the limit of small slope ($Kx_0\gg 1$) the density and kinetic energy in the surface region approach the values given by the Thomas and Fermi model:

$$\frac{\rho(x)}{\rho_0}=\left(\frac{x_0-x}{x_0}\right)^{\frac{3}{2}}, \tag{16}$$

$$\frac{t(x)}{t_0}=\left[\frac{\rho(x)}{\rho_0}\right]^{5/3}=\left(\frac{x_0-x}{x_0}\right)^{\frac{5}{2}}, \tag{17}$$

and

$$T_s=t_0\int_0^{x_0}\left[\left(\frac{x_0-x}{x_0}\right)^{\frac{5}{2}}-\left(\frac{x_0-x}{x_0}\right)^{\frac{3}{2}}\right]dx=-\frac{4}{35}x_0t_0. \tag{18}$$

A plot of the density corresponding to a falloff distance of 2.4 f is shown in Fig. 1 ($x_0=3.1$ f) obtained both from exact wave functions and from the Thomas-Fermi distribution, Eq. (16).

The kinetic surface energy in this limit is negative since the surface region contains an excess of low-energy particles. A plot of the kinetic surface energy as a function of x_0 is shown in Fig. 2. (The Fermi energy is taken as 32.5 Mev. Leveling off the potential at say 8 Mev above the Fermi energy would not appreciably change the results.)

Shown also in Fig. 2 is the contribution of the potential interaction to the surface energy. Calculations were made by Swiatecki for a Gaussian interaction. The

parameters are given in the caption and are chosen to reproduce the mean binding energy E_v and to approximate low-energy scattering data. Exact calculations were made in the limits $x_0 \to 0$ and $Kx_0 \gg 1$, and for several intermediate points. The minimum in the curve falls well below the observed surface energy of 18 to 26 Mev, but this example is only illustrative of the method. A more general study would seek to find a two-body effective (or pseudo-) potential which reproduces the observed surface energy and thickness as well as the mean binding energy. From such a potential, one might then hope to deduce other nuclear properties. Possible trial forms include velocity-dependent functions such as Brueckner's reaction matrix. The wave functions considered would then be reinterpreted as model wave functions, rather than true independent particle functions.

Self-consistent Hartree-Fock calculations have been carried out by Rotenberg[14] for the spherical nucleus $N=Z=92$. Yukawa and Gaussian wells were used, the latter yielding a somewhat more diffuse surface. Swiatecki's results are in general agreement with this work, although the latter displays specific shell effects.

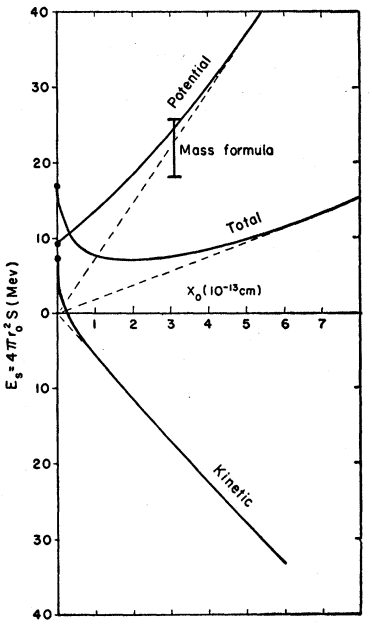

FIG. 2. Independent particle model: contributions to the surface energy in a semi-infinite well with sloping wall (after Swiatecki[13]). The kinetic energy is computed exactly. The potential energy is computed exactly in first order in the limits $x_0 \to 0$ and $Kx_0 \gg 1$, and for several intermediate points. The two-body interaction is a Gaussian of range 2.073 f. The strength of the even interaction is -42.94 Mev; the odd interaction is repulsive and 0.6 times the strength of the even. This interaction leads to a binding energy of -15.75 Mev and an equilibrium radius constant of $r_0 = 1.216$ f.

IV. STATISTICAL MODEL

In an attempt to apply methods which have proved very successful for electrons in atoms, Gombas[15] applied the statistical model to the nucleus. The energy is written in the form

$$E=\int\left\{\mathcal{E}_V(\rho)+\frac{1.81\hbar^2}{M}\rho^{5/3}+\frac{\hbar^2}{8M}\frac{(\nabla\rho)^2}{\rho}\right\}d\tau, \quad (19)$$

where the first term in the integrand is the interaction energy density computed as a function of density from plane waves. The second term is the Fermi kinetic energy. The third term is an inhomogeneity correction to the kinetic energy first suggested by Weizsäcker.[16] (The term is in error, see Sec. V.) Gombas worked with finite, spherically symmetric nuclei. By choosing a functional form for the density, the energy of the nucleus can be minimized (subject to keeping the number of nucleons fixed) by varying parameters in the density function. Gombas tried several two-body potentials, but worked especially with Yukawa wells of range given by the mesonic mass. Saturation was obtained by exchange. The strength of the interaction was left as an adjustable parameter.

Gombas was able to fit binding energies (including surface effects) over the entire range of nuclear masses fairly well with only one adjustable parameter. His density distributions, however, were unrealistic. He obtained Gaussians for light and medium weight nuclei, and slightly flattened Gaussians for the heavy nuclei. The central density was an order-of-magnitude greater than observed. The general method has much value, however, if not approached from first principles.

V. SEMIEMPIRICAL STATISTICAL MODEL

A statistical model of the nucleus utilizing several pieces of experimental data has been studied by Berg and the author.[17,18] No explicit assumptions about nucleon-nucleon forces are made, and details of the many-body wave function are not required. Semiempirical approaches had been used previously[19–21] to study the interior distribution of nuclear matter, and subsequently[22,23] to study surface phenomenon. This section follows the development of Berg and Wilets.[17,18]

A. Equal Numbers of Neutrons and Protons

Consider first a nucleus with $N=Z$ and neglect Coulomb forces. It is assumed that the energy of the nucleus can be written in the form

$$E=\int\left\{\mathcal{E}(\rho)+\frac{\zeta\hbar^2}{8M}\frac{(\nabla\rho)^2}{\rho}\right\}d\tau. \quad (20)$$

The integrand is to be considered the beginning of an

[14] M. Rotenberg, Phys. Rev. **100**, 439 (1954).
[15] P. Gombas, Acta Phys. Hung. **1**, 239 (1952); **2**, 223 (1952); **3**, 105, 127 (1953); Gombas, Mágori, Molnár, and Szabo, Acta Phys. Hung. **4**, 267 (1955); Gombas, Szépfalusy, and Mágori, Acta Phys. Hung. **7**, 251 (1957).
[16] C. F. von Weizsäcker, Z. Physik **96**, 431 (1935).
[17] R. A. Berg and L. Wilets, Phys. Rev. **101**, 201 (1956).
[18] L. Wilets, Phys. Rev. **101**, 1805 (1956).
[19] E. Wigner, Bicentennial Symposium, University of Pennsylvania (1940).
[20] E. Feenberg, Phys. Rev. **59**, 593 (1941); Revs. Modern Phys. **19**, 239 (1947).
[21] W. J. Swiatecki, Proc. Phys. Soc. (London) **A63**, 1208 (1950).
[22] D. P. Hale and R. D. Present, Phys. Rev. **104**, 448 (1956).
[23] T. H. R. Skyrme, Phil. Mag. Ser. 8, **1**, 1043 (1956); F. Villars (private communication).

expansion for the energy density of nuclear matter in powers of various derivatives of the density.

The first term in the integrand, $\mathcal{E}(\rho)$, represents the energy density of a uniform nuclear medium. It includes both potential and kinetic energies and should, in principle, be derivable from a complete solution of the infinite many-body problem. We are primarily interested in the following properties of $\mathcal{E}(\rho)$ (see Fig. 3). The energy per particle, $\mathcal{E}/\rho$, as a function of density, has a minimum at the observed density of nuclear matter, and the value at minimum is the mean binding energy per particle, E_v [Coulomb and symmetry effects are accounted for separately in the mass formula (3)]. The curvature of $\mathcal{E}/\rho$ at the minimum is related to nuclear compressibility K, defined by

$$K=\frac{R^2}{A}\frac{\partial^2 E}{\partial R^2}\bigg|_{R_0}=9\rho^2\frac{\partial^2(\mathcal{E}/\rho)}{\partial\rho^2}\bigg|_{\rho_0}, \tag{21}$$

where R_0 is the normal radius and ρ_0 is the normal (central) density of the nucleus. The quantity K is not readily obtainable from experiment, and is considered a parameter of the theory. Its value can then be fixed by comparison with experimental predictions of the model. Further details in the form of $\mathcal{E}(\rho)$ are not important for present considerations, since at low density the energy is governed by the gradient term.

The appearance of a gradient term arises from two sources. Firstly, as proposed by Weizsäcker,[16] there is a correction to the (Fermi) kinetic energy when the density is not constant. Although Weizsäcker's derivation of the inhomogeneity correction term, $(\hbar\nabla\rho)^2/(8M\rho)$, has been shown to be in error,[24] the form of the term is such as to give qualitatively meaningful results; these results can be made quantitative if the term is reduced by a factor between $\frac{1}{2}$ and $\frac{1}{8}$, depending on the details of the potential. Secondly, a gradient term should also arise from effects of the finite range of nucleon-nucleon forces. The form of such a term could be $(\nabla\rho)^2$ or $\nabla^2\rho$ multiplied by a function of density. Since the energy cannot depend on the sign of the gradient, first derivatives should not enter. A $\nabla^2\rho$ term can be converted to $(\nabla\rho)^2$ (plus other terms) by partial integration. The form chosen to simulate both effects was that of the Weizsäcker inhomogeneity correction term multiplied by the single adjustable constant ζ.

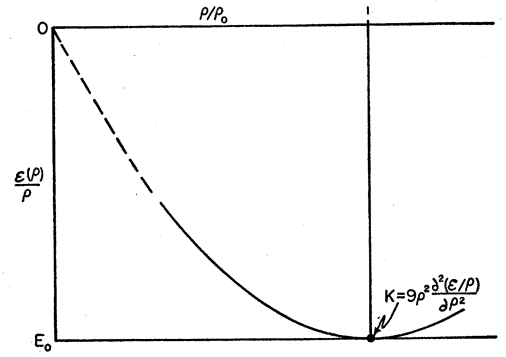

FIG. 3. Energy per particle as a function of density. The curve is schematic, representing the form given by Eq. (27), $n=1$. The main features of the curve are the minimum at $\rho=\rho_0$, the value E_0 at ρ_0, and the curvature at ρ_0 which is related to compressibility. Low density behavior of the curve is not important to the B-W theory.

[24] R. A. Berg and L. Wilets, Proc. Phys. Soc. (London) **A68**, 229 (1955).

It should be stressed that the energy density can include effects due to correlations, velocity dependent forces, etc.

Minimization of the energy (20) with respect to ρ, subject to the condition that the total number of particles $A=\int\rho d\tau$ remains fixed, leads to the differential equation

$$\frac{-\zeta\hbar^2}{2M}\nabla^2 u+\frac{\partial\mathcal{E}}{\partial\rho}u=E_0 u, \tag{22}$$

where $u=\rho^{\frac{1}{3}}$ and E_0 is a Lagrangian multiplier (see below).

Although Eq. (22) has the appearance of a Schroedinger equation, it is nonlinear since the "effective potential" $\partial\mathcal{E}/\partial\rho$ depends on ρ (or u). Furthermore, $\partial\mathcal{E}/\partial\rho$ should not be interpreted as a potential since it includes kinetic energy.

For the case of the plane surface, we seek solutions of the form

$$\begin{aligned} &u\to u_0=\rho_0^{\frac{1}{3}},\quad u'\to 0,\quad u''\to 0,\quad \text{as } x\to-\infty,\\ &u\to 0,\quad u'\to 0,\quad u''\to 0,\quad \text{as } x\to+\infty. \end{aligned} \tag{23}$$

Equation (22) can then be integrated once to yield

$$\frac{\zeta\hbar^2}{2M}(u')^2=\mathcal{E}(\rho)-E_0u^2. \tag{24}$$

The following integrability conditions can be derived from Eqs. (22) to (24):

$$\begin{aligned} &\frac{\partial(\mathcal{E}/\rho)}{\partial\rho}\bigg|_{\rho_0}=0,\\ &E_0=\frac{\partial\mathcal{E}}{\partial\rho}\bigg|_{\rho_0}=\frac{\mathcal{E}}{\rho}\bigg|_{\rho_0}, \end{aligned} \tag{25}$$

which are restatements of the saturation conditions. We note that E_0 is equal to both the energy of the "last" particle and to the mean energy per particle, E_v.

The surface energy, defined by Eq. (7), can be shown to be given by

$$S=\frac{\zeta\hbar^2}{M}\int_{-\infty}^{\infty}(u')^2dx=\int_0^{\rho_0}\left\{\frac{\zeta\hbar^2}{2M}\left(\frac{\mathcal{E}}{\rho}-E_0\right)\right\}^{\frac{1}{2}}d\rho. \tag{26}$$

Equal contributions to the surface energy come from

the gradient term and from the loss of binding energy of particles in the surface region.

The differential equation (22) or (24) can be integrated analytically for particular choices of $\mathcal{E}(\rho)$. A convenient one-parameter family of functions is

$$\mathcal{E}(\rho)=|E_0|\rho\left\{-2\left(\frac{\rho}{\rho_0}\right)^{1/n}+\left(\frac{\rho}{\rho_0}\right)^{2/n}\right\}, \tag{27}$$

which clearly satisfy the saturation conditions (25). To the extent that we are only interested in the properties of $\mathcal{E}(\rho)$ discussed in the foregoing, we think of the members of this family as differing only in the compressibility,

$$K=18|E_0|/n^2. \tag{28}$$

The density functions are given by

$$\rho/\rho_0=\{1+\exp[x/(na)]\}^{-n}, \tag{29}$$

where $a^2=\zeta\hbar^2/(8M|E_0|)$. The surface energy is

$$S=\frac{\rho_0}{n+1}\left|\frac{E_0\zeta\hbar^2}{2M}\right|^{\frac{1}{2}}, \tag{30}$$

and the surface thickness

$$D=\left|\frac{\zeta\hbar^2}{8ME_0}\right|^{\frac{1}{2}}\lambda(n)=\frac{S}{|E_0|\rho_0}\left(\frac{n+1}{2}\right)\lambda(n), \tag{31}$$

where

$$\lambda(n)=n\ln\left\{\frac{(0.1)^{-1/n}-1}{(0.9)^{-1/n}-1}\right\}\approx 4.39+2.89(n-1). \tag{32}$$

Equations (28), (30), and (31) relate $E_0=E_v$, ρ_0, S, D, and K.

Values of the compressibility K (along with n and ζ) derived from three different mass formulas are given in Table I (see caption for discussion of an error in reference 17). The value of K obtained by Brueckner and Gammel[25] using Gammel-Thaler[26] hard core potentials is 172 Mev. This number agrees well with the value derived from Green's mass formula but is considerably less than that derived from Cameron's formula.

B. Unequal Numbers of Neutrons and Protons

The extension of the above methods to finite, spherical nuclei, including Coulomb effects, with unequal numbers of neutron and protons has also been investigated.[18] The coupled differential equations corresponding to (22) are

$$-\frac{\zeta\hbar^2}{2M}\nabla^2 u_\mu+\frac{\partial\mathcal{E}}{\partial\rho_\mu}u_\mu=E_0u_\mu, \tag{33}$$

where the index μ stands for n (neutrons) or p (protons). The Lagrangian multiplier has been set equal to the same value for both neutrons and protons to insure stability against beta decay; i.e., the binding energies of the last neutron is equal to that of the last proton.

The energy density function $\mathcal{E}(\rho_n,\rho_p)$ is assumed to be of the form

$$\mathcal{E}(\rho_n,\rho_p)=\mathcal{E}(\rho)+k(\rho_n-\rho_p)^2+V_c\rho_p. \tag{34}$$

The function $\mathcal{E}(\rho)$, where $\rho=\rho_n+\rho_p$, is taken equal to the $\mathcal{E}(\rho)$ of the previous subsection.

The second term on the right-hand side of (34) is identified with nuclear symmetry energy, which can arise from several effects: (a) The Fermi kinetic energy can be written in the form $(1.81\hbar^2/M)\rho^{5/3}[1+\frac{5}{6}(\rho_n-\rho_p)^2/\rho^2+\cdots]$. (b) Because of the antisymmetrization of the wave function, nucleons have more bonds with unlike rather than with like nucleons. Thus when a neutron excess occurs, the protons experience greater potential than the neutrons. (c) If the effective (or pseudo-) potential is velocity dependent, the excess nucleons will experience less potential because of their greater kinetic energy. These three effects are probably not independent. Although the coefficient k should probably be density dependent, it was evaluated near normal density from the semiempirical mass formula (3):

$$k=E_{v,\,sy}/\rho_0. \tag{35}$$

At low density, only the gradient term is important anyway.

The third term on the right-hand side of Eq. (34) represents the Coulomb energy (taken here as given by the proton interacting with an external potential).

Numerical integration of the coupled differential equation (33) leads to neutron and proton distributions which are very similar (Fig. 4). The proton distribution is slightly more peaked near the surface than the

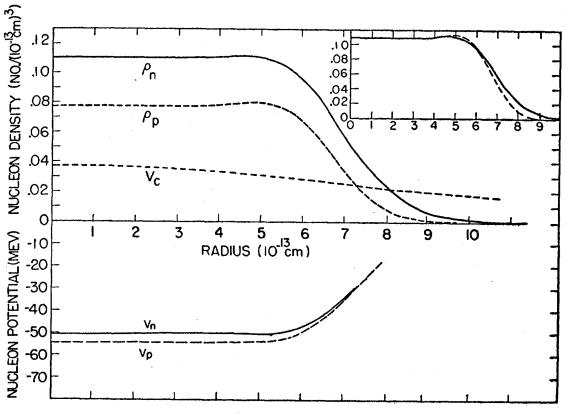

FIG. 4. Neutron and proton densities and potentials.[17] The graph illustrates the type of densities and potentials obtained from integrating Eq. (33) in spherical symmetry. The example depicted is for an hypothetical nucleus of $A=225$ and $Z=93$. The potentials were derived using an effective mass approximation ($M^*=0.6$ M) and were not carried to low density since the potential energy is not significantly approximated at low density.

[25] K. A. Brueckner and J. L. Gammel, Phys. Rev. **109**, 1023 (1958).

[26] Gammel, Christian, and Thaler, Phys. Rev. **105**, 311 (1957); J. L. Gammel and R. M. Thaler, Phys. Rev. **107**, 1337 (1957).

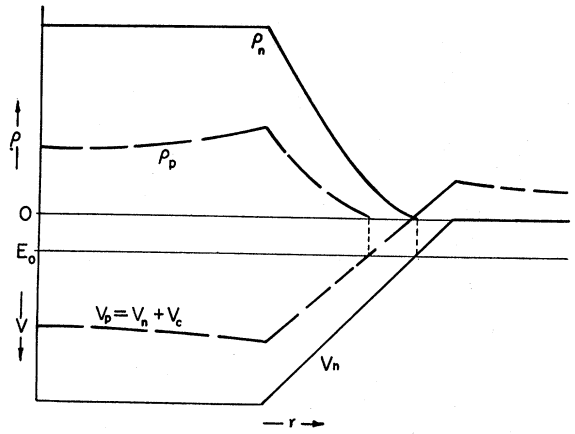

FIG. 5. Schematic representation of the Johnson-Teller effect. The proton potential is taken to be the neutron potential plus the Coulomb potential. This leaves the classical turning point of the fastest proton inside that of the fastest neutron. The densities are given in Thomas-Fermi approximation, and the proton distribution is seen to lie inside the neutron distribution. The effect is enhanced when barrier penetration is included, since the proton barrier is higher than that of the neutrons. The effect is strongly decreased with the inclusion of symmetry energy, which cuts the difference between the neutron and proton potentials by roughly one-half.

neutron distribution, but the neutrons have a slightly longer tail. At the midpoint of the distributions, the radius associated with the neutrons is about 0.2 f larger than that associated with the protons.

This result is to be contrasted with earlier speculations about neutron and proton distributions. Earlier it was believed that protons would be concentrated in a shell near the surface of the nucleus because of Coulomb repulsion. Johnson and Teller[27] pointed out another consequence of Coulomb forces operating in the reverse direction: Consider an independent particle model in which neutrons and protons experience the same potential except for Coulomb forces (Fig. 5). Then the proton potential will lie above the neutron potential by the amount of the Coulomb potential. The neutrons and protons fill their respective wells to the same maximum energy E_0. Because of finite surface thickness, the proton potential crosses the maximum energy E_0 inside the neutron crossing. In the Thomas-Fermi model this would confine the protons inside the neutrons. Furthermore, the Coulomb repulsion acts as a barrier which restricts proton penetration beyond the crossing. These effects are related to neutron excess (which is also a consequence of Coulomb forces) and may also be interpreted as due to the greater penetration into the surface region of the more energetic particles (neutrons).

The Johnson-Teller effect is modified by symmetry energy. In the language of the independent particle model, the protons experience a deeper nuclear potential than the neutrons, and it turns out that the difference in in total potential is cut to about half the Coulomb potential.[18,28] This, coupled with variation of the Coulomb potential inside the nucleus (which does tend to concentrate protons at the surface), results in only a small difference between the radii.

The conclusions of this subsection are mainly directed to heavy nuclei near the stable valley. If one considers mirror nuclei ($N=Z$) including Coulomb effects, the protons would lie outside the neutrons. Finally, nuclei with greater neutron excess would find the neutrons extending beyond the protons.

VI. NUCLEAR POTENTIALS

The methods of Sec. V avoid separation of the energy into potential and kinetic parts. A more detailed nuclear model is required for that. The independent particle models for nuclear levels (shell model) and scattering (optical model) provide the framework within which the nuclear potentials can be discussed.

A general consequence of any independent particle model which leads to saturation is that the potential is a nonlinear function of density. In fact, the potential must eventually increase less rapidly than the kinetic energy, which varies as $\rho^{\frac{2}{3}}$. This means that the potential falls off less rapidly with radial distance than the density, leading to a larger potential radius.

Calculations[18] have been made using the semi-empirical energy densities of the previous sections. The effective mass approximation was introduced so as to allow identification of the potentials for normal mass nucleons:

$$V_\mu = \frac{M^*}{M}\left[\frac{\partial \mathcal{E}}{\partial \rho_\mu} - \frac{19.14\hbar^2}{M^*}\rho^{\frac{2}{3}}\right]. \tag{36}$$

The nuclear part of the neutron and proton potentials were similar in depth and radius, each extending about 0.7 f beyond the matter distributions at half-maximum.

Brueckner[29] has used a local reaction matrix (as well as two-body potentials in first order) to calculate the nonlinearity effect. He has found the potential to extend about 0.5 f further than the matter.

In addition to the nonlinearity effect is a specific finite-range effect. In first approximation, this can be estimated by folding the effective nucleon potential, $v_e(|\mathbf{r}-\mathbf{r}'|)$, into the density distribution[29]

$$V(\mathbf{r}) = \int \rho(\mathbf{r}')v_e(|\mathbf{r}-\mathbf{r}'|)d\mathbf{r}'. \tag{37}$$

If the range of the effective two-body potential were independent of density, the only effect would be a thickening potential surface with respect to the density surface (as was seen to be the case for the effect of the proton size on charge distribution). But the range of the

[27] M. H. Johnson and E. Teller, Phys. Rev. **93**, 357 (1954).

[28] Ross, Mark, and Lawson, Phys. Rev. **102**, 1613 (1956).

[29] K. A. Brueckner, Phys. Rev. **103**, 1121 (1956).

effective potential increases with decreasing density, which results in a longer tail.

Combining the nonlinearity and finite-range effects, Brueckner[29] estimated the potential rms radius to be about 1.35 f greater than that of the density. This is more than adequate to explain the experimental difference of (1.0 ± 0.3) f.

The foregoing arguments show how, given a density function, the potential may be seen to extend farther. From the point of view of self-consistency, it is encouraging that given a potential, the density can be shown to lie inside. Swiatecki's[13] independent particle model illustrates the point. In the Thomas-Fermi approximation, the mean density radius lies $0.6x_0$ inside the classical turning point for the last particle [cf. Eq. (16)]. Noting that the potential rises another 8 Mev beyond the turning point, the difference between the mean potential and density radii becomes $[0.1+\frac{1}{2}(8/32.5)]x_0 = 0.223x_0$, or inserting Swiatecki's value $x_0=3.1$ f, the difference becomes 0.7 f.

VII. MANY-BODY PROBLEM

The most successful approach to the nuclear many-body problem has been that of Brueckner and coworkers. The infinite nuclear problem has been calculated numerically by Brueckner and Gammel[25] using the empirical two-body potentials of Gammel and Thaler.[26] The minimum in the binding energy curve was found to fall at very nearly the observed density and at very nearly the observed energy.

Although the nuclear surface problem as defined in Sec. II is infinite, it has many of the complications of the finite problem. The finite problem has been formulated in Brueckner theory,[30] but complexities have prohibited numerical calculations.

Brueckner, Gammel, and Weitzner[31] have proposed an approximation which uses the reaction matrix of the infinite medium, calculated as a function of density. It appears to be most convenient to treat the finite problem and the surface problem in configuration space. The reaction matrix then has the form of a nonlocal potential, $(\mathbf{r}|t|\mathbf{r}')$, which is evaluated at the local density. The nuclear problem is then solved by the Hartree self-consistent approximation. The basic assumptions are that the correlations in regions of varying density are the same as in infinite media of the same (local) density, and that the range of correlations is short compared with (say) the surface thickness.

There remains some question as to whether the reaction matrix is sufficient for handling nuclear matter considerably below normal density. Higher order clusters become more important as the density is decreased. For example, at very low density, the matter would separate into clusters of alpha particles, oxygen nuclei, or, most preferably, iron nuclei. Such correlations do not come out of the reaction matrix, which treats fully only two-body correlations. (Correlations of order higher than two are not important near normal density.)

In spite of some unanswered questions, it seems clear that the Brueckner-Gammel-Weitzner proposal could provide a fundamental advance in our understanding of the surface problem from first principles.

[30] K. A. Brueckner and C. A. Levinson, Phys. Rev. **97**, 1344 (1955); R. J. Eden, Proc. Roy. Soc. (London) **A235**, 408 (1956); J. Goldstone, Proc. Roy. Soc. (London) **A239**, 267 (1957); H. A. Bethe, Phys. Rev. **103**, 1353 (1956).

[31] Brueckner, Gammel, and Weitzner, Phys. Rev. (to be published).